www.amlett.com, www.vbripress.com/aml, DOI: 10.5185/amlett.2015.5713 Published online by the VBRI press in 2015

SHI induced thermoluminescence properties of sol-gel derived $Y_2O_3:Er^{3+}$ nanophosphor

N.J. Shivaramu[1], B.N. Lakshminarasappa[1*], K.R. Nagabhushana[2], Fouran Singh[3]

[1]*Department of Physics, Jnanabharathi Campus, Bangalore University, Bangalore 560 056, India*
[2]*Department of Physics (S & H), PES University, 100 feet Ring Rd., BSK 3rd Stage, Bangalore 560 085, India*
[3]*Inter University Accelerator Centre, P.O. Box No. 10502, New Delhi 110 067, India*

[*]Corresponding author. Tel: (+91) 9448116281; E-mail: bnlnarasappa@rediffmail.com

Received: 17 October 2014, Revised: 16 December 2014 and Accepted: 24 December 2014

ABSTRACT

Nanocrystalline erbium doped yttrium oxide ($Y_2O_3:Er^{3+}$) was synthesized by the sol-gel technique using citric acid as complexing agent. The synthesized samples were characterized by X-ray diffraction (XRD), Field emission scanning electron microscope (FE-SEM) techniques for phase-purity and microstructure. Er^{3+} doped Y_2O_3 crystallizes in cubic phase with an average crystallite size of 24.3 nm. The pellets of $Y_2O_3:Er^{3+}$ were irradiated with 100 MeV swift Si^{8+} ions with fluence in the range of 3×10^{11} - 3×10^{13} ions cm^{-2}. Three well resolved thermoluminescence (TL) glows with peaks at ~422, 525 and 620 K were observed in Er^{3+} doped Y_2O_3 samples. It was observed that the TL intensity was found to increases with increasing Er^{3+} concentration up to 0.4 mol% in Y_2O_3 and thereafter it decreases with further increase of Er^{3+} concentration. Also, the intensity of low temperature TL glow peak (~422 K) increases with increasing ion fluence up to 1×10^{12} ions cm^{-2} and decreases with further increase of ion fluences. The TL trap parameters were calculated by glow curve shape method and the deconvoluted glows were exhibit of second order kinetics. Copyright © 2015 VBRI press.

Keywords: Sol-gel synthesis; swift heavy ion; XRD; FE-SEM; thermoluminescence.

N.J. Shivaramu, completed his M. Sc. in Condensed Matter Physics during 2009 at Bangalore University, Bangalore, India. He is currently pursuing Ph.D. in SHI induced luminescence at Bangalore University under IUAC, (UFR) project.

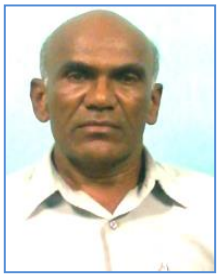

B.N. Lakshminarasappa obtained his M.Sc degree in Solid State Physics from Sri Venkateswara University, M.Ed from the University of Madras and PhD from Bangalore University, India. He has joined the Department of Physics, Bangalore University, Bangalore and involved both teaching as well as Research and as Professor from 2009. His topics of interest in Condensed Matter Physics include synthesis of crystalline, nanophase and thin films of inorganic and metal oxide materials; characterization, Luminescence and Defects studies. Some of the phosphors materials are found to be useful in low to high energy radiation dosimetry while others find applications in lamp industry. He has supervised eight PhD candidates and six M.Phil students. He has about 150 research publications which include about 50 in refereed international journals. He has been reviewer for couple of international journals and adjudicator for PhD thesis of different universities.

K.R. Nagabhushana received his M.Sc. from Bangalore University, India and Ph.D in experimental condensed matter Physics from the same university, in 2009. The experiments for PhD work were done in collaboration with Inter University Accelerator Center, New Delhi, India. His research interests are in the area of Materials Physics. These include development of nanophosphors for LED's and radiation dosimetry, as well as analysis of specific materials, phase transition and defects under swift heavy ion irradiation.

Introduction

Nanomaterials find a wide range of applications due to their unique chemical, physical, electrical, magnetic, optical and mechanical properties. Moreover, rare-earth ions in different host lattices prompted the development of rare-earth luminescent materials for lamps, cathode ray tubes, dosimetry, scintillators, bio sensors and white light-emitting diodes **[1-5]**. Yttrium oxide (Y_2O_3) possesses high refractory properties with melting point of ~2723K and thermal conductivity of 33Wm^{-1} K^{-1}. It is a suitable material for photonic waveguide due to its high band gap (5.72 eV), with a very high refractive index (~2) and a wide transmission range (280–8000 nm), a low phonon cut-off energy, which leads to high luminescence efficiency **[6-8]**.

Y_2O_3 is a best promising host material for Er^{3+} because Er_2O_3 and Y_2O_3 have the same crystal structures with very similar lattice constants, and Y^{3+} and Er^{3+} trivalent ions have nearly the same ionic radii **[9,10].**

Swift heavy ions (SHI) have been exploited by researchers in different ways in the field of materials science. The energy of the ion, ion fluence and ion species greatly affect the properties of phosphors. SHI is very useful for modification of the properties of thin films and surface of bulk solids. It penetrates deep into the target material; lose their energy predominately through inelastic interactions with the target electrons. The resulting intense electronic excitation can produce a narrow trail of permanent damage along the ion path called ion track **[11, 12].** Also, it produces point defect and defect clusters. These defects, affect the luminescence properties of materials. Thermoluminescence (TL) is a powerful technique to study damage creation under SHI. It is used to identify the nature of defects and their thermal stability in crystalline solids. TL is highly structure-sensitive, simple, a reliable technique and has wide applications in personal monitoring, archeological age determination of pottery, geological dating, etc **[13, 14].** Recent studies indicate that luminescent nanomaterials have potential applications in dosimetry caused by ionizing radiations for the measurements of high doses using the TL technique **[15].** It may be noted that nanophosphors are in use as high-dose detectors for ionizing radiation. In the present work, structural and TL properties of 100 MeV Si^{8+} irradiated Y_2O_3:Er^{3+} nanophosphors synthesized by sol-gel technique at low temperature are reported and discussed in details.

Experimental

Erbium doped yttrium oxide was synthesized by sol-gel technique using yttrium (III) oxide (Y_2O_3, Aldrich, 99.99% trace metals basis, Saint Louis, USA), erbium (III) oxide (Er_2O_3, Aldrich, 99.99% trace metals basis, Saint Louis, USA), citric acid anhydrous ($C_6H_8O_7$, Merck, 99.5% purity GR, Mumbai, India) and nitric acid (HNO_3, Merck, 65% purity GR, Mumbai, India) as ingredients. All the chemicals were directly used without any purification. The ratio of citric acid to Y^{3+} was considered as 2.0 **[16-18]**. Stoichiometric amount of yttrium oxide, erbium oxide were dissolved with dilute nitric acid to get yttrium nitrate and erbium nitrate. The yttrium nitrate was dissolved in 50 ml of double distilled water and then the solution was refluxed at room temperature for 3 hour. Erbium nitrate was added to yttrium nitrate precursor solution and the solution was refluxed at 343 K for 2 hrs and then citric acid was added slowly which acts as a chelating agent. Again, it was refluxed at 348-353 K for 5 hrs. During refluxing, the solution slowly evaporated and turned into a reddish brown gel. The gel was dried at 383 K to overnight in an oven to obtain powder. The powder was ground in an agate pestle-mortar and finally annealed at 973 K for 2 hrs to remove the impurities if any **[18].** Pellets of 1 mm thick and 5 mm diameter were prepared by taking 30 mg of the sample with 4% of poly vinyl alcohol solution (binder)**[19]** and by applying a pressure of 4.0 MPa using a homemade pellatizer. These pellets were annealed at 1173 K for 2 hrs in a muffle furnace to remove the deformations and binding agent impurities if any left behind. The annealed pellets were irradiated with 100 MeV swift Si^{8+} ions having beam current of 2 pnA for fluences in the range $3\times10^{11} - 3\times10^{13}$ ion cm^{-2} using 15 UD Pelletron at Inter University Accelerator Centre (IUAC), New Delhi, India **[20]**. The samples were mounted on glass slide of 10 cm length, 2.5 cm width and 2 mm thickness. The glass slide was carefully fixed on a copper target ladder using double sided sticky tape. The ion beam was magnetically scanned on a 1cm×1cm area of samples surfaces for uniform irradiation at room temperature. Four pellets were exposed at a time for the same fluence.

The unirradiated (pristine) and SHI irradiated samples were characterized by powder X-ray diffraction [Bruker AXS -model D-8 X-ray diffractometer] using 1.5406 Å CuK_α radiations. The morphology of the pristine sample was studied by a field emission scanning electron microscope [MIRA II LMH from TESCAN]. The TL glow curves of the SHI irradiated Y_2O_3:Er^{3+} samples were recorded in the temperature range of 323–673 K at a heating rate of 5 Ks^{-1} using Harshaw TLD reader (Model 3500). All experiments were performed at room temperature.

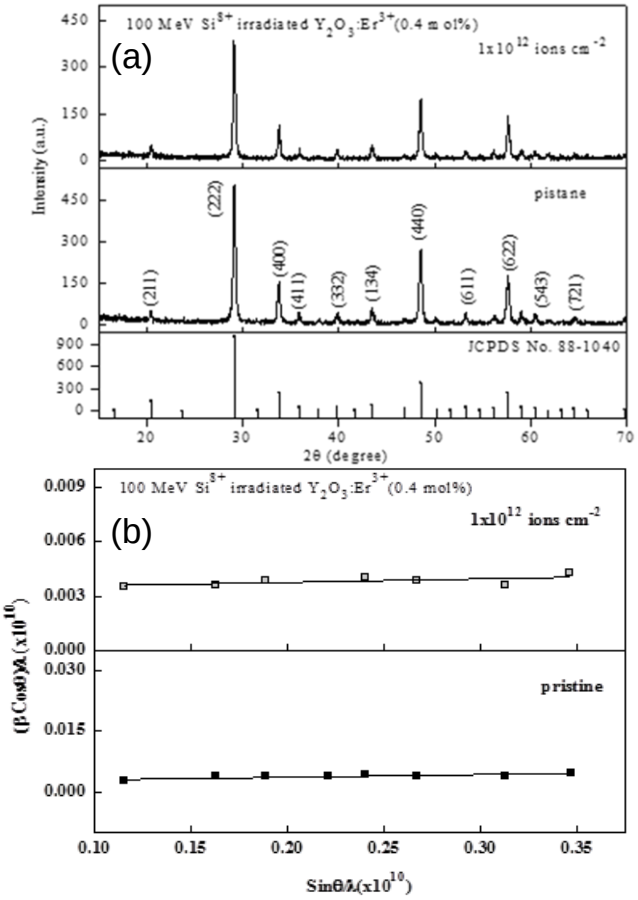

Fig. 1. (a) XRD patterns of pristine and 100 MeV swift Si^{8+} ion irradiated Y_2O_3:Er^{3+} and (b) W-H plot of pristine and 100 MeV swift Si^{8+} ion irradiated Y_2O_3:Er^{3+}.

Results and discussion

Fig. 1(a) shows the XRD pattern of pristine and 100 MeV swift Si^{8+} irradiated Y_2O_3:Er^{3+} for the fluence of 1×10^{12}

ions cm^{-2}. The XRD pattern of pristine and irradiated samples were found to be cubic crystal system with space group $Ia\bar{3}$ (JCPDS: No: 88-1040) **[21]**. All the diffraction peaks have been indexed correspond to bixbyite (C-type) crystalline phase of yttrium oxide. It was found that the diffraction peak intensity of irradiated sample decreases when compared to that of pristine one. This might be due to the creation of a large number of defects. This indicates that after ion irradiation Er^{3+} doped Y_2O_3 sample do not change the phase, but the degree of crystallinity decreases **[22]**.

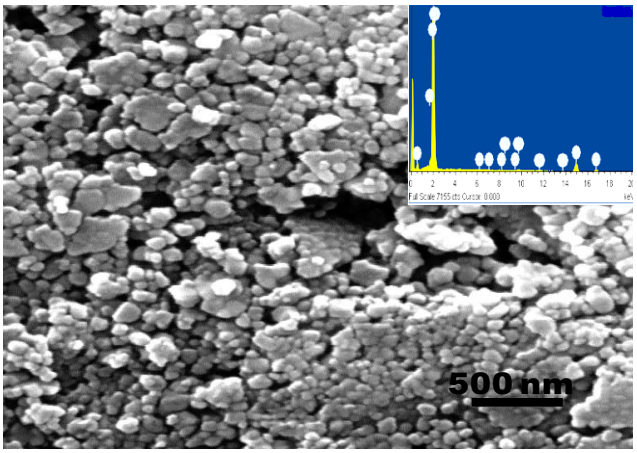

Fig. 2. FE-SEM micrograph and Inset Fig.: EDS of sol-gel synthesized nanocrystalline $Y_2O_3:Er^{3+}$.

The structural parameters such as crystallite size (D), inter-planar spacing (d), lattice constant (a), cell volume (V), particle density (D_x), dislocation density (δ) and lattice strain (ε) were calculated from XRD data and tabulated in **Table 1**. The crystallite size (D) is calculated using Scherrer equation **[23].**

$$D = \frac{0.9\lambda}{\beta\cos\theta} \qquad (1)$$

where, 'λ' is the wavelength of X-rays (1.5406 Å), 'β' is full width at half maxima (FWHM) and 'θ' is the Bragg angle. The average crystallite size was found to be 24.3 nm for pristine and 23.6 nm for ion irradiated samples. Significant strains were associated with nanoparticles because a large number of surface atoms have unsaturated in co-ordinations system. The lattice strain and crystallite size are estimated using Williamson Hall (W-H) equation **[24, 25]** and given in the **Table 1**.

$$\frac{\beta\,\mathrm{Cos}\theta}{\lambda} = \frac{1}{D} + \frac{4\varepsilon\mathrm{Sin}\theta}{\lambda} \qquad (2)$$

where, 'ε' is the lattice strain.

Fig. 1 (b) shows the plot of (βCosθ)/λ along y-axis versus (Sin θ)/λ along x-axis. The average crystallites size and lattice strain are found to be 35.0 nm and 0.169 % for pristine and 29.5 nm and 0.182 % for ion irradiated samples. The dislocation density and lattice strain were found to increase after SHI irradiation and it might be due to SHI induced lattice disorder in the $Y_2O_3:Er^{3+}$ nanophosphor **[23, 25]**.

Fig. 2 shows the FE-SEM image of 1173 K annealed $Y_2O_3:Er^{3+}$. It is observed from the **Fig. 2**, that, the particles are spherical in shape and are agglomerated. Also porosity was observed due to the large amount of gases produced during synthesis. The average grain size is estimated to be 35 mm. The energy dispersive X-ray spectroscopy (EDS or EDX) technique has proved to be a powerful tool to obtain the chemical composition. Inset of **Fig. 2** shows the presence of Y, O, Er elements in the synthesized sample.

Table 1. XRD structural parameters of pristine and 100 MeV swift Si^{8+} irradiated $Y_2O_3:Er^{3+}$.

Sample	Crystallite size, D (nm)		Lattice constant, a (Å)	Cell Volume, V ($Å^3$)	Density, ρ ($gm\ cm^{-3}$)	Dislocation Density, δ ($x10^{15}$)	Inter-planar space, d in at (222) (Å)	Lattice strain, ε (%)	
	Debye Scherrer	W-H method						W-H method	Calculated
Pristine	24.3	35.0	10.617	1196.76	5.01	1.69	3.065	0.169	0.146
Irradiated 1×10^{12} (ions cm^{-2})	23.6	29.5	10.601	1191.35	5.04	1.79	3.058	0.182	0.148

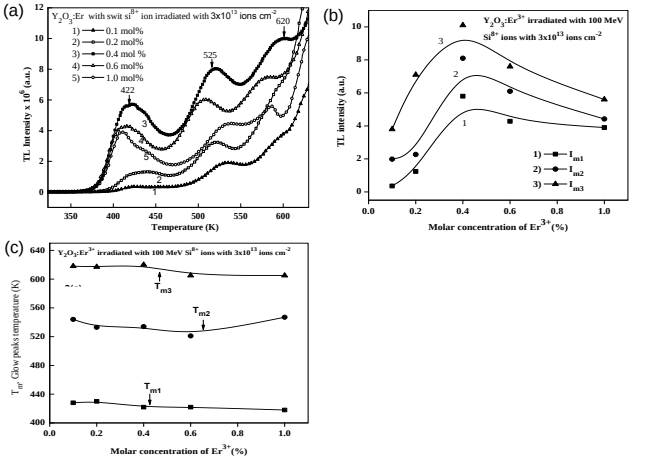

Fig. 3. (a) TL glow curves of 100 MeV swift Si^{8+} ion $3x10^{13}$ ion cm^{-2} irradiated with $Y_2O_3:Er^{3+}$, (b) variation of TL glow peaks (I_m) intensity and (c) TL glow peaks temperature (T_m) with molar concentration of Er^{3+}.

Fig. 3(a) shows the TL glow curves of $Y_2O_3:Er^{3+}$ (0.1-1.0 mol%) irradiated with 100 MeV Si^{8+} for a fluence of 3×10^{13} ions cm^{-2}. Three prominent TL glows with peaks at ~422, 525 and 620 K were observed and these might be due to oxygen vacancies (O_2^-), F and F^+ centers respectively **[26]**. The variation of TL intensity (I_m) and glow peaks temperatures (T_m) are plotted as a function of the concentration of Er^{3+} are shown in **Figs. 3(b)** and **(c)**. It is observed that the TL glow peak intensity increases with increase of Er^{3+} up to 0.4 mol% and further it decreases with increasing concentration of Er^{3+}. This might be due to concentration quenching behavior **[27].** Impurity present, even in ppm levels in the material will significantly affect the luminescence yield. If the impurity concentration is too high, they may act as self-quenchers by causing non-radiative cross transitions resulting in quenching of the luminescence yield. Manjunatha et al., reported thermoluminescence properties of 100MeV Si^{7+} swift heavy ions and UV irradiated $CdSiO_3:Ce^{3+}$ nanophosphor. They observed concentration quenching effects at 5mol% of Ce^{3+}

in ion irradiation and 3mol% of Ce^{3+} doped $CdSiO_3$ for UV exposure respectively **[28]**. Numan salah et al., reported TL of γ-irradiated LiF: Mg, Cu, P. They observed that optimum impurity concentration was found to be 0.4, 0.002 and 0.85 mol% of Mg, Cu and P, respectively.

This might be due to the impurity aggregation and acting as self-quenchers **[29].** In present work, as Er^{3+} concentration increases in the host, the distance between Er^{3+} ions decreases, resulting the pairs or clustering of Er^{3+} ions which may reduce TL intensity. However, its glow peak temperatures were not perturbed much as can be seen from **Fig. 3(c)**.

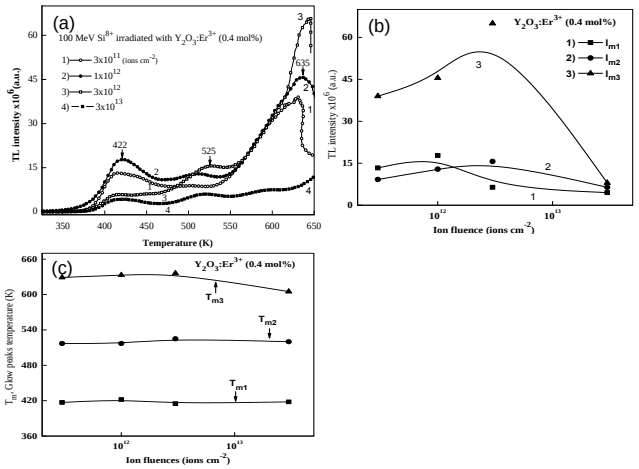

Fig. 4. (a) TL glow curves of 100 MeV swift Si^{8+} ion irradiated nanocrystalline $Y_2O_3:Er^{3+}$, (b) variation of TL glow peaks (I_m) intensity and (c) TL glow peaks temperature (T_m) with ion fluences.

Fig. 4(a) shows the TL glow curves of 100 MeV Si^{8+} ion irradiated $Y_2O_3:Er^{3+}$ (0.4 mol%) for fluence in the range from 3×10^{11} to 3×10^{13} ions cm^{-2} in the temperature range of 323–650 K. These well resolved glows with peak at ~422, 525 and 635 K were recorded at a heating rate of 5 Ks^{-1}. Further, the results indicate that creation of trapping centers increase with increase of ion fluence. The TL intensity at the glow peaks are plotted as a function of fluence as shown in **Fig. 4 (b)**. It is observed that the TL glow peak intensity increases with Si^{8+} fluence and reaches a maximum at ~1×10^{12} ions cm^{-2} for a glow peak at 422 K (T_{m1}), at 3×10^{12} ions cm^{-2} for the glow peaks at 525 (T_{m2}) and 620 K (T_{m3}). Further, it decreases with increasing ion fluence. Also, it is observed that the low temperature glow peak (T_{m1}) reaches very fast saturation level, when compared to other high temperature glow peaks (T_{m2} and T_{m3}). It might be due to creations of additional trapping centers. Normally, released electrons from the trapping centers recombine with holes at the luminescence centers resulting to TL signal. Low temperature glow peak exhibit a shallow traps level in band gap of material, therefore, with increasing ion fluence, the shallow level traps increases, leading to complex/ cluster defects, which leads to reduction in TL signal with ion fluence.

A typical TL glow curves were deconvoluted using Origin 8.0 software **[18]** and five prominent TL glows with peaks at 419, 446, 513, 588 and 636 K for 0.4 mol% of Er^{3+} were well resolved as can be seen from **Fig. 5(a)**. The theoretically obtained TL glow curves are well fitted with the experimental data and the quality of fitting is described by figure of merit (FOM). The fits are considered to be adequate when the FOM values are below 5% **[30]**. The FOM for the present curve fitting is 0.8%, which indicates that a good agreement between theoretically generated and experimentally recorded TL glow curves. In order to be able to understand the nature of the traps formed in $Y_2O_3:Er^{3+}$ under SHI irradiation, we have employed the analysis of trapping parameters. The trapping parameters of the above deconvoluted TL glow curves are calculated using the glow curve shape method (modified by Chen) **[14]**.

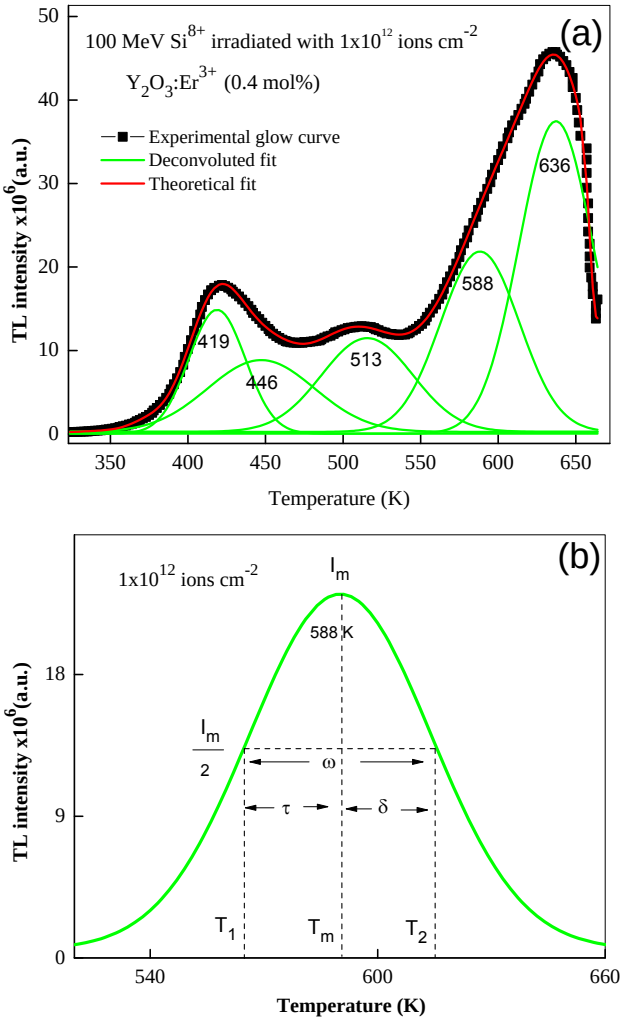

Fig. 5. (a) Deconvoluted TL glow curves in 100 MeV swift Si^{8+} ion irradiated $Y_2O_3:Er^{3+}$ and (b) parameters used in the glow curve shape method (modified by Chen).

The order of kinetics of glow curves are calculated by measuring the symmetry (geometrical) factor μ_g~0.50 ($\mu_g=\delta/\omega$). The values of τ, δ and ω as indicated in **Fig. 5 (b)** are calculated. Here, 'τ' is the low-temperature half width of the glow curve, i.e. $\tau = T_m - T_1$, 'δ' is the high-temperature half width of the glow curve, i.e. $\delta = T_2 - T_m$ and 'ω' is the full width of the glow peak at its half height i.e. $\omega = T_2 - T_1$. From the values of the geometrical factor, it is clear that the above five glow peaks obey the second order kinetics indicating the occurrence of retrapping phenomena. Other trapping parameters such as activation energy (E),

frequency factor (s) and trap density (n_o) of the luminescence centers are calculated using various method based on the glow curve shape **[14, 31].**

General formulae for calculation of trap depth (E) by various glow curve shape methods are given by:

$$E_\gamma = C_\gamma\left(k\frac{T_m^2}{\gamma}\right) - b_\gamma(2kT_m) \quad \text{(Chen)} \quad (3)$$

$$E_\gamma = C_\gamma\left(\frac{kT_m T_1}{\gamma}\right) \quad \text{(Grossweiner)} \quad (4)$$

$$E_\gamma = C_\gamma\left(\frac{kT_m^2}{\gamma}\right) \quad \text{(Luschik)} \quad (5)$$

where γ is τ, δ or ω. Thus, trap depth is calculated by averaging the E_τ, E_δ and E_ω values, c_γ and b_γ are constant for all three methods for second order kinetics **[10, 14]**. The calculation of trapping parameters by various glow curve shape methods shows a close agreement as seen in **Table 2**.

Table 2. TL Trap parameters of 100 MeV swift Si^{8+} irradiated Y_2O_3: Er^{3+}.

Method	T_{m1} (419K)		T_{m2} (446K)		T_{m3} (513K)		T_{m4} (588K)		T_{m5} (636K)	
	E (eV)	s (s^{-1})	E (eV)	s (s^{-1})	E (eV)	s (s^{-1})	E (eV)	s (s^{-1})	E (eV)	s (s^{-1})
Chen	1.02	6.2×10^{11}	0.76	8.1×10^{7}	1.12	2.4×10^{10}	1.42	3.5×10^{11}	1.07	4.4×10^{7}
Grossweiner	1.03	8.3×10^{11}	0.78	1.4×10^{8}	1.14	3.9×10^{10}	1.44	5.3×10^{11}	1.10	7.8×10^{7}
Luschik	1.09	4.6×10^{12}	0.84	7.3×10^{8}	1.21	2.0×10^{11}	1.52	2.7×10^{12}	1.18	3.6×10^{8}

The trap density for deconvoluted glow with peaks at 419, 446, 513, 588 and 636 K are found to be 3.8×10^7, 4.2×10^7, 4.5×10^7, 8.6×10^7 and 22.0×10^7 cm^{-3}. And the effective atomic number (Z_{eff}) has been defined as **[32]**.

$$Z_{eff} = \sqrt[m]{\sum_i a_i Z_i^m} \quad (6)$$

where 'a_i' is the fractional electron content of element i with atomic number Z_i. The value of 'm' will typically range from 3 to 4, with 3.5 a reasonable value **[32]**. Z_{eff} of Y_2O_3:Er^{3+} compound has been calculated for various different mol% of Er as $Er_{0.001}$ = 36.49, $Er_{0.002}$ = 36.84, $Er_{0.004}$ = 37.18, $Er_{0.006}$ = 37.52, $Er_{0.008}$ = 37.85 and $Er_{0.01}$ = 38.16.

Conclusion

Y_2O_3:Er^{3+} nanophosphors have been synthesized by the sol-gel technique at low temperature. The synthesized sample shows cubic phase upon annealing at 1173 K with the average crystallite size of 24.3 nm. The FE-SEM image of Y_2O_3:Er^{3+} indicated that, particles are spherical in nature and their size are found to be ~35 nm. Three TL glows with peaks at ~422, 525 and 620 K were recorded with SHI irradiation. TL glow peaks intensity increases with concentration of Er^{3+} and it reaches a maximum at 0.4 mol% and further it decreases with increasing concentration of Er^{3+}. In SHI irradiated samples, the TL glow (422 K) peak intensity (I_{m1}) increases up to a fluence of 1×10^{12} ions cm^{-2} then it decreases with further increase of ion fluence. Deconvoluted TL glow curves exhibited second order kinetics since the retrapping of electron is high. TL glow curves were analyzed by various glow curve shape methods shows a close agreement. It is suggested that Y_2O_3:Er^{3+} nanophosphor suitable for radiation dosimetry applications of high energy radiation. In continuation of the present work, it is proposed to investigate photoluminescence (PL) and ionoluminescence (IL) behavior of the samples irradiated with SHI. PL and IL will through light on the local symmetry of the emitting atom structural defects.

Acknowledgements

The authors express their sincere thanks to Dr. D.K. Avasthi, Materials Science Group, Dr. S.P. Lochab, Health Physics Group, Inter University Accelerator Centre, New Delhi, India for their constant encouragement and help during the experiment. Also, one of the authors (N.J.S.) is grateful to Inter University Accelerator Centre, New Delhi, for providing fellowship under UFR (No. 48303) scheme.

Reference

1. Anh, T.; Benalloul, P.; Barthou, C.; ThiKieu, G. L.; Vu, N.; Minh, L. *J. Nanomater*. **2007**, *2007*, 1. **DOI:** 10.1155/2007/48247
2. Yan, B.; Su, X.Q. *Opt. Mater.*, **2007**, *29*, 547. **DOI:** 10.1016/j.optmat.2005.08.050
3. Nagpure, I.M.; Subhajit Saha.; Dhoble, S.J. *J. Lumin.*, **2009** *129*, 898. **DOI:** 10.1016/j.jlumin.2009.03.034
4. Patel, D.N.; Hardy, L. a.; Smith, T.J.; Smith, E.S.; Wright, D.M.; Sarkisov, S. *J. Lumin*. **2013**, *133*, 114. **DOI:** 10.1016/j.jlumin.2011.12.015
5. Zhong, J.; Liang, H.; Han, B.; Su, X.Q.; Tao, T. *Chem. Phys. Lett.*, **2008**, *453*, 192. **DOI:** 10.1016/j.cplett.2008.01.032
6. Liu, X.; Li, Y.; Wang, X. *Mater. Lett.*, **2006**, *60*, 1943. **DOI:** 10.1016/j.matlet.2005.12.059
7. Fukabori, A.; Sekita, M.; Ikegami, T.; Iyi, N.; Komatsu, T.; Kawamura, M.; Suzuki, M. *J. Appl. Phys.*, **2007**, *101*, 043112. **DOI:** 10.1063/1.2709867
8. Huang, H.; Sun, X.; Wang, S.; Liu, Y.; Li, X.; Liu, J.; Kang, Z.; Lee, S.T. *Dalton Trans.*, **2011**, *40*, 11362. **DOI:** 10.1039/c1dt11553g
9. Mao, Y.; Huang, J.Y.; Ostroumov, R.; Wang, K.L.; Chang, J.P. *J. Phys. Chem. C*, **2008**, *112*, 2278. **DOI:** 10.1021/jp0773738
10. Som, S.; Chowdhury, M.; Sharma, S. K. *J. Mater. Sci.*, **2013**, *49*, 858. **DOI:** 10.1007/s10853-013-7769-8
11. Kluth, P.; Schnohr, C.; Pakarinen, O.; Djurabekova, F.; Sprouster, D.; Giulian, R.; Toulemonde, M. *Phy.Revie. Lett.*, **2008**, *101*, 175503. **DOI**:10.1103/PhysRevLett.101.175503
12. Szenes, G. *Phy. Revi. B*, **1999**, *60*, 3140. **DOI:** 10.1103/PhysRevB.60.3140
13. Mckeever, S.W.S. Thermoluminescence of Solids, Cambridge University Press: Cambridge, 1985. **DOI**:10.1017/CBO9780511564994
14. Furetta, C. Handbook of Thermoluminescence, World Scientific Publishing: Singapore, 1937. **DOI:** 10.1142/9789812564863_0002-0014
15. Zhydachevskii, Y.; Syvorotka, I.I.; Vasylechko, L.; Sugak, D.; Borshchyshyn, I.D.; Luchechko, A.P.; Vakhula, Y.I.; Ubizskii, S.B.; Vakiv, M.M.; Suchocki. A. *Opt. Mater.*, **2012**, *34*, 1984. **DOI:** 10.1016/j.optmat.2011.12.023
16. Dupont, A.; Parent, C.; Le Garrec, B.; Heintz, J. *J. Solid State Chem.*, **2003,** *171*, 152. **DOI:** 10.1016/S0022-4596(02)00202-5
17. Chen Weifan; Li Fengsheng; Liu Leili; Yongxiu. *J. Rare Earths*, **2006**, *24*, 543. **DOI:** 10.1016/S1002-0721(06)60160-9
18. Lakshminarasappa, B.N.; Shivaramu, N.J.; Nagabhushana, K.R.; Singh, F. *Nucl. Instruments Methods Phys. Res. Sect. B Beam Interact. with Mater. Atoms*, **2014**, *329*, 40. **DOI:** 10.1016/j.nimb.2014.02.128
19. Shibani Das. Study of composition behavior of binders and the effect of bender type on strength and density of Alumina samples (B.Tec thesis), 2011.
20. Kanjilal, D.; Chopra, S.; Narayanan, M.M.; Indira S. Iyer.; Vandana Jha.; Joshi, R.; Datta, S.K. *Nucl. Instr. Meth. A*, **1993**, *328*, 97. **DOI:** 10.1016/0168-9002(93)90610-T

21. Liu, T.; Xu, W.; Bai, X.; Song, H. *J. Appl. Phys*. **2012,** *111*, 064312. **DOI:**10.1063/1.3694767
22. Gaboriaud, R.J.; Jublot, M.; Paumier, F.; Lacroix, B. *Nucl. Instruments Methods Phys. Res. Sect. B Beam Interact. with Mater. Atoms*, **2013,** *310*, 6. **DOI:** 10.1016/j.nimb.2013.05.014
23. Som, S.; Dutta, S.; Kumar, V.; Swart, H.C.; Sharma, S.K. *J. Lumin*. **2014,** *146*, 162. **DOI:** 10.1016/j.jlumin.2013.09.058
24. Khorsand Zak, a.; Abd. Majid, W.H.; Abrishami, M.E.; Yousefi, R. *Solid State Sci.*, **2011,** *13*, 251. **DOI:** 10.1016/j.solidstatesciences.2010.11.024
25. Shivaramu, N.J.; Lakshminarasappa, B.N.; Nagabhushana, K.R.; Singh, F.; *Radiat. Meas.*, **2014,** *71*, 518**.** **DOI:** 10.1016/j.radmeas.2014.03.027
26. Singh, V.; Rai, V.K.; Ledoux-Rak, I.; Watanabe, S.; Gundu Rao, T.K.; Chubaci, J.F.D.; Badie, L.; Pelle, F.; Ivanova, S. *J. Phys. D. Appl. Phys.*, **2009,** *42*, 065104. **DOI:** 10.1088/0022-3727/42/6/065104
27. Dubey, V.; Kaur, J.; Agrawal, S.; Suryanarayana, N.S.; Murthy, K.V.R. *Superlattices Microstruct*., **2014**, *67*, 156. **DOI:** 10.1016/j.spmi.2013.12.026
28. Manjunatha, C.; Sunitha, D.; Nagabhushana, H.; Singh, F.; Sharma, S.C.; Chakradhar, R.P.S.; Nagabhushana, B.M. *J. Lumin.*, **2013,** *134*, 358. **DOI:** 10.1016/j.jlumin.2012.08.020
29. Salah, N.; Sahare, P.D.; Rupasov, A. A. *J. Lumin*., **2007,** 124, 357. **DOI:** 10.1016/j.jlumin.2006.04.004
30. Som, S.; Dutta, S.; Chowdhury, M.; Kumar, V.; Kumar, V.; Swart, H.C.; Sharma, S.K. *J. Alloys Compd.*, **2014.** *589*, 58. **DOI:** 10.1016/j.jallcom.2013.11.182
31. Shivaramu, N.J.; Lakshminarasappa, B.N.; Nagabhushana, K.R.; and Singh, F. *Radiat. Eff. Defects Solids*, **2014,** *169***,** 696. **DOI:** 10.1080/10420150.2014.922561
32. Bos, a. J. *Radiat. Meas.*, **2001**, *33*, 737. **DOI:** 10.1016/S1350-4487(01)00094-4

